CHIN. PHYS. LETT. Vol. 38, No. 8 (2021) 083301

Revisiting Laser-Intensity-Dependent Ionization and Fragmentation of C_{60}

D. P. Dong(董达谱)[1,2], B. H. Yang(杨博涵)[1,2], D. B. Qian(钱东斌)[1,2*], W. C. Zhou(周文长)[1,2], S. F. Zhang(张少锋)[1,2], and X. Ma(马新文)[1,2*]

[1]*Institute of Modern Physics, Chinese Academy of Sciences, Lanzhou 730000, China*
[2]*University of Chinese Academy of Sciences, Beijing 100049, China*

(Received 1 April 2021; accepted 22 June 2021; published online 2 August 2021)

We revisit the laser-intensity-dependent ionization and fragmentation yields of C_{60} molecules irradiated by 25-fs, 798-nm laser pulses based on the approach in which photoions are measured via a velocity map imaging spectrometer working in a time-sliced mode. This approach dramatically improves the signal-to-background ratio compared to those using a simple (traditional) time-of-flight mode (spectrometer), and thus allows us to measure the laser-intensity dependences down to a previously untouched region, which is expected to provide new insights into the intense-field ionization and fragmentation of C_{60}. Indeed, we find that the saturation intensities for C_{60} ionizations and the onset intensity for C_{60} fragmentation are much lower than those reported in previous experiments. Furthermore, the derived saturation-intensity dependence on charge distribution demonstrates the validity of the over-the-barrier ionization using a conducting sphere model.

DOI: 10.1088/0256-307X/38/8/083301

The intense-field laser ionization and fragmentation of large molecules are of considerable current interest (see, e.g., Refs. [1–3]). With its unique highly symmetric structure and its large number of electronic and nuclear degrees of freedom, the C_{60} molecule has proven to be a particularly instructive model for studying such processes.[4–6] In contrast to the case of small molecules, at laser intensities below the threshold of saturation ionization, C_{60} fragmentation already starts to compete with ionization due to a strong coupling of electronic excitation energy into vibrational degrees of freedom.[7,8] In this situation, in order to understand the mechanisms of intense-field excitation, ionization, and fragmentation for such a complex molecule, it is of vital importance to measure the dependences of the ionization and fragmentation yields on the laser intensity covering the range where one expects to see the actual transition from almost "pure" ionization to predominant fragmentation.

During the past few decades, many efforts have been devoted to the measurements of the laser-intensity-dependent ionization and fragmentation yields of C_{60} molecules irradiated by femtosecond (fs) laser pulses, using a traditional time-of-flight mass spectrometer (TOFMS).[7,9–11] As a typical example, Tchaplyguine *et al.*[7] studied the ionization and metastable fragmentation of C_{60} with 795 nm laser pulses of 35 fs duration. They demonstrated that at the laser intensities below the onset of fragmentation and the saturation of C_{60}^{+} signal, single ionization is a direct multiphoton process; at laser intensities beyond the onset of double ionization, there is considerable metastable fragmentation. However, some undesirable background effects exist when the traditional approach is used to detect a specific ion species, such as the disturbances of thermal noise from the microchannel plate (MCP) stack and of other ion species having the same TOF as the targeted species. This generally causes a poor signal-to-background ratio, which hinders an experimental test of the laser-intensity dependences of C_{60} ionization and fragmentation down to a lower intensity regime where actual intensity thresholds appear. As a result, the thresholds for ionization saturations and fragmentation onset of C_{60} may be over-estimated when the traditional TOFMS is used as a diagnostic tool.

In this Letter, we apply an alternative approach to re-examine the laser-intensity-dependent ionization and fragmentation of C_{60} molecules irradiated by short laser pulses. This approach is based on the measurements of the time-sliced photoion image using a velocity map imaging spectrometer (VMIS). It is demonstrated that such an approach can achieve the identification of ion species having the same TOF and effectively reduce the disturbance of thermal noise from the MCP to the ion signal, and therefore dramatically improve the signal-to-background ratio in the detection of a specific ion species. Based on the advantages, we achieve the measurements on the ionization and fragmentation yields of C_{60} irradiated by 25-fs, 798-nm laser pulses in a low intensity range which has not been explored before. The results provide new in-

Supported by the National Key R&D Program (Grant No. 2017YFA0402300), and the National Natural Science Foundation of China (Grant Nos. 11974359 and U1632143).
*Corresponding authors. Email: qiandb@impcas.ac.cn; x.ma@impcas.ac.cn
© 2021 Chinese Physical Society and IOP Publishing Ltd

sights into the intensity thresholds for the ionization saturations and fragmentation onset of C_{60} molecules.

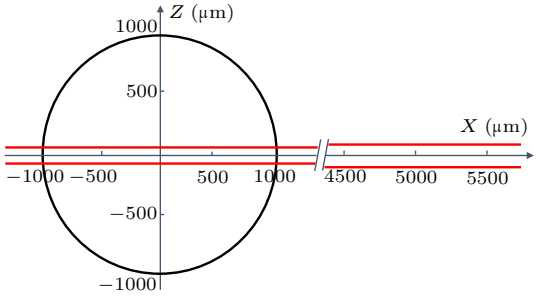

Fig. 1. Geometry of the interaction region between the laser beam (along the X axis, red lines) and molecular beam (black circle) crossing at right angles.

Experiment and Data Analysis. The experimental setup, excepting the fs laser system, was described in detail in our earlier studies on the interaction of ns laser pulses with C_{60} molecules.[12–14] Briefly, we carried out the experiments using a VMIS designed following the principle proposed by Eppink and Parker.[15] The C_{60} powder was evaporated in an oven at a temperature of 515 ± 5 ℃. The oven was located below the ion optics of the spectrometer. The C_{60} molecules escaped from the oven through an orifice (diameter, 1 mm), pass through two collimation apertures (diameter, 1 mm) separated by 60 mm, and generate a thin molecular beam. The distance between the last collimation aperture and the interaction point was set at 60 mm to realize a beam diameter of about 2 mm in the interaction region. We used a Ti:sapphire fs laser to excite the C_{60} molecules. The laser consists of a Kerr-lens mode locked oscillator and an amplifier based on the chirped pulse amplification technique.[16,17] We measured the pulse duration (FWHM) to be 25 fs using a technique of frequency-resolved optical gating. The central wavelength of the laser radiation was 798 nm. The near Gaussian laser beam was focused on the well-collimated molecular beam by a lens with 30 cm focal length. The focal spot diameter (FWHM) was measured by imaging the beam waist on a CCD camera after laser beam intensity is appropriated and attenuated, to be 70 ± 10 μm. The laser beam cross sections at the waist were thus $(4 \pm 1) \times 10^{-5}$ cm^2. One μJ of pulse energy therefore corresponded to a light intensity within the focal spot of $(1.1 \pm 0.4) \times 10^{12}$ W/cm^2. The laser intensity was changed by a set of thin neutral density filters. The geometry of the interaction region between laser beam and the well collimated C_{60} beam is sketched in Fig. 1. The black circle (diameter, 2 mm) is the cross section of C_{60} beam and the red lines are the projection of laser waist (width, 0.07 mm) in scale. Since the Rayleigh length of the laser beam in the present setup is about 10 mm, we may consider with sufficient accuracy the molecules to be excited by a cylindrical beam, thus constituting a well-defined geometry of the excitation/ionization region.

The Photek's VID240 detector system, consisting of a MCP stack and a phosphor screen assembly coupled with a CCD camera, was used in the VMIS. Before experiments, we have taken great care to check the linear responses of the detector to the input photoion flux using an approach established recently,[18] including the linearity of the MCP stack and of the phosphor screen module. To record one TOF spectrum, a constant high voltage was applied to the MCP and the ion signals from the MCP were acquired via a digital phosphor oscilloscope (TDS 3034C, Tektronix Ltd.) using a rolling average mode. In other words, the TOF spectrum is recorded under the conditions of the VMIS working in a traditional TOFMS mode. To obtain a position image of photoions corresponding to a selected TOF window, a high-voltage switch having a delay with respect to the laser pulse was applied for gating the MCP. In this case, ion signals from the MCP were converted to luminescence by the phosphor screen which was captured by a CCD camera to generate a time-sliced photoion image. In the following section we will demonstrate that such an VMIS working in the time-sliced imaging mode has a wonderful signal-to-background ratio in detecting specific ion species.

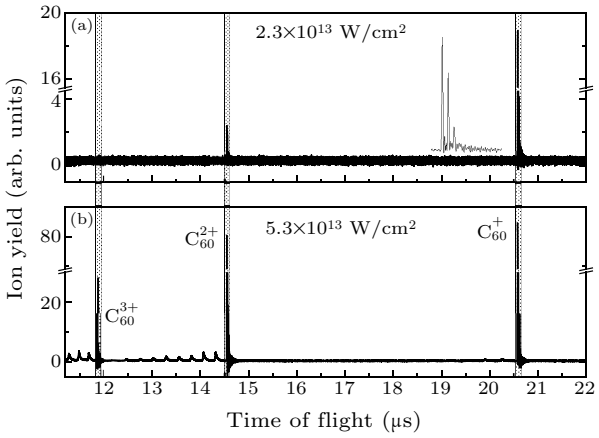

Fig. 2. Typical TOF spectra measured at two different laser intensities: (a) 2.3×10^{13} W/cm^2 and (b) 5.3×10^{13} W/cm^2. The inset in (a) shows that the resolution of our spectrometer enables isotope identification in the C_{60} molecule, which is mainly attributed to the use of a well-collimated C_{60} beam.

Taking the laser intensities of 2.3×10^{13} and 5.3×10^{13} W/cm^2 as examples, typical TOF spectra of photoions are shown in Fig. 2. In the case of 5.3×10^{13} W/cm^2, the strong peaks at the TOFs of 20.58 μs, 14.55 μs and 11.88 μs are attributed to stable C_{60}^+, C_{60}^{2+} and C_{60}^{3+} ions produced by single, double, and triple ionizations, respectively. In addition, a series of weak peaks related to charged fragments C_{60-2m}^{q+} (q = 1–3; m = 1, 2, ...) are faintly visi-

ble. Such weak peaks imply that the intensity value of $(5.3 \pm 1.9) \times 10^{13}\,\mathrm{W/cm^2}$ calibrated by us is very close to the threshold for the fragmentation onset estimated by a traditional TOFMS. A previous study[7] using 795 nm laser pulses with a duration of 35 fs presented that the fragmentation onset occurs at around $7 \times 10^{13}\,\mathrm{W/cm^2}$, which agrees well with the implication from our data. We are thus confident that the present intensity calibration is reliable. Conversely, at $2.3 \times 10^{13}\,\mathrm{W/cm^2}$, those peaks corresponding to stable C_{60}^{3+} and C_{60-2m}^{q+} ions cannot be observed in the TOF spectrum, as if indicating that the intensity of $2.3 \times 10^{13}\,\mathrm{W/cm^2}$ is below the thresholds for the fragmentation onset and triple ionization of the C_{60} molecule.

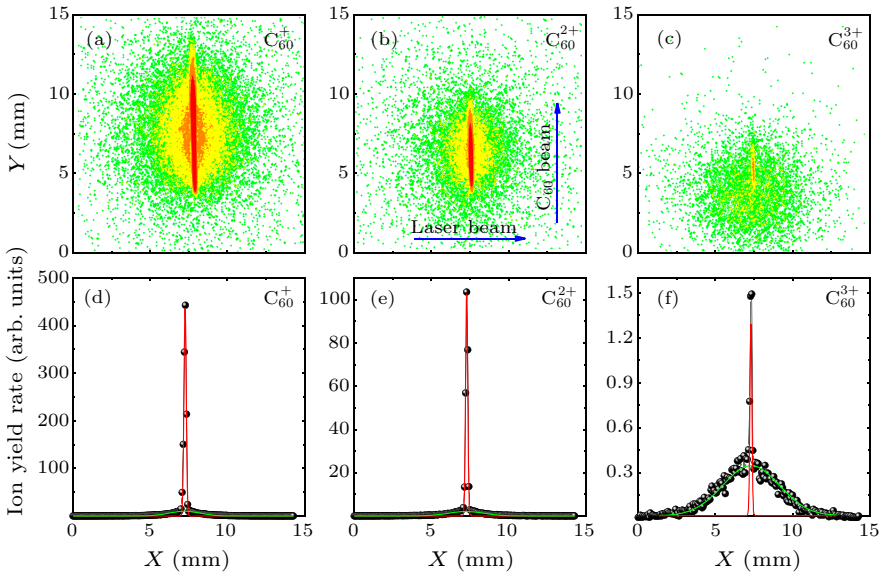

Fig. 3. (a)–(c) Time-sliced photoion images recorded in the selected TOF windows (the shaded areas in Fig. 2) at $2.3 \times 10^{13}\,\mathrm{W/cm^2}$. The directions of C_{60} beam and laser beam are indicated in frame (b). (d) and (e) Projections of images (a)–(c) onto X-axis, solid spheres: experimental data; solid lines: fits with Gaussian functions; red solid lines correspond to contributions of stable C_{60}^{q+} ions, and green solid lines correspond to contributions of charged fragments.

In Figs. 3(a)–3(c) we display the position images of C_{60}^{q+} (q = 1–3) ions at $2.3 \times 10^{13}\,\mathrm{W/cm^2}$ obtained by the VMIS working in the time-sliced imaging mode. The time-sliced photoion images were recorded using a detector gate width of 0.1 μs triggered at the TOF's of 20.53, 14.50, and 11.83 μs, respectively. The images detected in the selected time windows (the shaded areas in Fig. 2) were accumulated up to 6000, 12000, and 18000 laser shots, respectively. As pointed out in a previous work,[12] the position of each ion along X-axis (the direction of the laser beam) on the detector was uniquely related to its transverse velocity with respect to the direction of the molecular beam. The projections of Figs. 3(a)–3(c) onto the X-axis are presented in Figs. 3(d)–3(f). In each projected spectrum, the photoion distribution consists of two distinct components, narrow and broad profiles. The needle-like narrow component is the C_{60}^{q+} ions produced by ionization, which are stable until reaching the detector. The broad component is attributed to a mixture contribution of those charged fragments C_{60-2m}^{q+} caused by delayed C_2 and electron emissions of metastable neutral and ionized C_{60} during flight paths which have a TOF located in the selected time windows. It is noted that the observed broad components indicate the occurrence of fragmentation at such a low intensity ($2.3 \times 10^{13}\,\mathrm{W/cm^2}$). Surprisingly, stable C_{60}^{3+} signals are unambiguously detected, where, of course, the accompanying metastable fragmentation dominates as shown in Figs. 3(c) and 3(f).

The results mentioned above clearly demonstrate that a much better performance can be achieved using this approach to detect a specific ion species with a VMIS working in the time-sliced imaging mode than the method working in the simple time-of-flight mode. First, the signal-to-background ratio was significantly improved, because the phosphor screen cannot be effectively lightened by the thermal noise from the MCP stack and therefore reduces the disturbance of the thermal noise to ion signal. It has been confirmed by the fact that there is almost no background signal outside the PS region reached by photoions. Second, the measurement of the time-sliced photoion image allows the identification/extraction of a targeted species from the others located in the same time window according to their position distribution features. Such advantages are expected to provide an opportunity for studying the intense-field laser ionization and frag-

mentation of large molecules, especially those having complex decay mechanisms similar to C_{60} molecules, at low intensities down to a previously untouched regime. Employing this approach, we measure the laser intensity-dependent ionization and fragmentation of C_{60} by recording a series of time-sliced photoion images for C_{60}^{q+} (q = 1–3) with the same time windows as shown in Fig. 2. The scanned intensity covered a range of (0.3–6.7) $\times 10^{13}$ W/cm^2. By fitting the narrow and broad components with Gaussian functions [see Figs. 3(d)–3(f)], we can obtain the yields of stable C_{60}^{q+} ions and the accompanying charged fragments within the corresponding time windows at various laser intensities.

Results and Discussion. The measured yields of stable C_{60}^{q+} (q = 1–3) ions as a function of the laser intensity are shown in Fig. 4. The yields in Figs. 4(a) and 4(b) are presented with standard log-log plots, it is obvious that the yields saturate at high intensity regions for all three charge states. It is an interesting but yet not completely solved puzzle to accurately determine the saturation intensities I_s for intense-field laser ionizations of larger molecules.[6,11,19–21] To derive the I_s values for the C_{60} ionizations from our measurements, we replot the yields using the lin-log plots in Figs. 4(c) and 4(d) as suggested by Hankin *et al.*,[19] and the best fits to the data are shown as the straight lines. The intersections of the fitted lines with the abscissa give the experimental derivations for the corresponding I_s values. The vertical dashed lines mark the derived I_s values, $(1.9 \pm 0.7) \times 10^{13}$ W/cm^2 for single ionization, $(2.8 \pm 1.0) \times 10^{13}$ W/cm^2 for double ionization, and $(4.1 \pm 1.5) \times 10^{13}$ W/cm^2 for triple ionization. The errors are given according to the uncertainty of the intensity calibration.

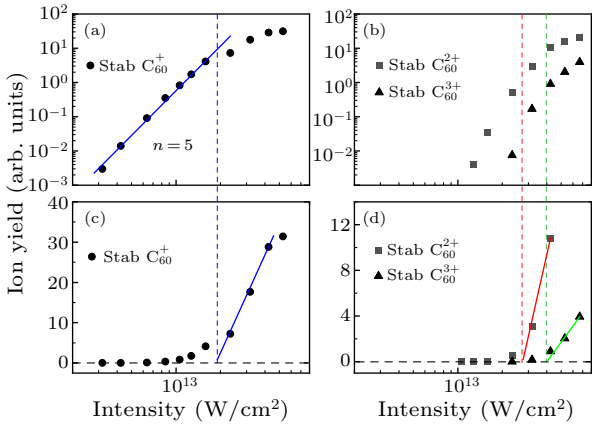

Fig. 4. Yields of stable C_{60}^{q+} (q = 1, 2, 3) ions as a function of laser intensity: (a) and (b) using log-log plots, (c) and (d) using lin-log plots. The best fits are shown as straight lines. The vertical dashed lines mark the saturation intensities.

It is well known that, below saturation, the dependence of the stable C_{60}^+ yield S_R on the laser intensity I can be represented by a power law, $S_R \propto I^n$, a feature of direct n-photon ionization process. From the best fitted straight line shown in Fig. 4(a), we obtain $n \approx 5$ for C_{60}^+, which provides evidence for direct multiphoton single ionization of C_{60} that requires five 798-nm photons to overcome the first ionization potential of 7.6 eV in an intensity range before saturation. The result agrees well with the power n deduced from similar measurements by Tchaplyguine *et al.*,[7] which gives additional support for the linear responses of our detection system.

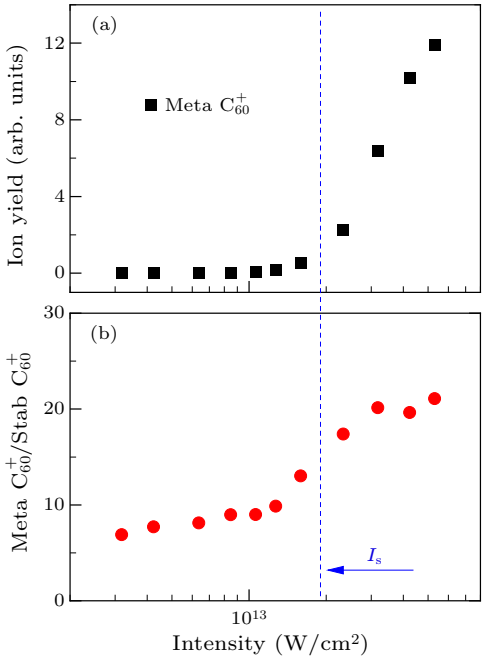

Fig. 5. Yields of charged fragments produced by metastable fragmentation and detected in the time window associated to single ionization of C_{60} (a), and the ratio of metastable fragmentation to stable C_{60}^+ (b) as a function of the laser intensity. The vertical blue dashed line marks the saturation intensity for the single ionization of C_{60}.

As mentioned above, we can distinguish the stable C_{60}^+ signals from the metastable fragmentation signals detected in a given time window. The yields of the metastable fragmentation associated to the single ionization measurements and the ratios of the metastable to stable contributions are plotted in Fig. 5. Our data shows that the metastable fragmentation seems to always accompany the occurrence of stable C_{60}^+ regardless of its saturation. However, the yield and the ratio both show a slow growth with increasing intensity before saturation (less than around 2×10^{13} W/cm^2) but a fast growth after saturation appears. Previous studies[11,22] demonstrated that the metastable fragmentation is a reliable indication for the existence of multielectron activation events. Considering that the "saturation" phenomena are usually interpreted as the number decrease of the neutral C_{60} molecules in the interaction region of the laser beam and the molec-

ular beam, a fast growth of multielectron activation events will inevitably cause the deviation of intensity-dependent stable C_{60}^{q+} yield from the simple model of direct multiphoton ionization. This is due to the fact that the multielectron activation process opens additional pathways to consume the neutral C_{60} molecules. Consequently, an abrupt growth of the metastable ratio at a laser intensity is expected to reflect the onset of the "saturation". Our data shown in Fig. 5 are in line with the expectation. Certainly, the pathways to be opened by multielectron activation are more complex than those thought, such as a statistical electron emission suggested by Hansen *et al.*[23]

In Fig. 6 the saturation intensities for C_{60}^{q+} ($q = 1$–3) derived by us are compared with earlier experimental results, obtained by combining traditional TOFMS with roughly-collimated molecular beams but using almost the same laser pulse duration and wavelength as this work.[9,11] One can find that the present I_s values are significantly smaller than the earlier data (a factor of around 5). It is well known that, at laser intensities higher than the saturation threshold, the stable C_{60}^{q+} yield starts to depend on the spatial profile of the laser beam and on the boundary of the interaction region where ions can be produced. In contrast to those previous experiments, a well-collimated molecular beam is used in the present experiment to limit the interaction region. This leads to a little variation in the on-axis intensity across the width of the molecular beam (see Fig. 1) and thus achieves similar outcomes as the intensity-selective scanning method proposed by Hansch and Woerkom,[24,25] which uses a pinhole at the front of the flight tube to select specific ion-production regions. Therefore, our experiment permits the observations of some subtle structures that could not be seen in the ion versus intensity plots obtained using roughly collimated molecular beams, because of the use of a "thin" molecular beam to minimize the masking effects from the focal region expansion with increasing intensity. As a result, such low saturation intensities derived here should be attributed to the fact that the data in Fig. 4 depict relative "clean" transitions of intensity-dependent C_{60}^{q+} yield from direct multiphoton ionization to saturation.

It should also be noted that the authors of Refs. [9,11] used a reflectron TOFMS to measure the laser-intensity-dependent ionization and fragmentation yields of C_{60}. This is an alternative approach to separate the "stable" C_{60}^{q+} ions from ions that decay from metastable states. "Stable" and "metastable" here are relative terms and depend on the timescale of the experiment. The flight time in the reflectron experiments is usually longer than in the linear experiments and therefore the stable species in Refs. [9,11] are more stable since they survive for longer time. It is therefore difficult to make a precisely quantitative comparison between the present study and the two earlier studies. However, if the present experiment would be performed using a reflectron TOFMS working in the TOF mode aided by a time-sliced imaging function, the saturation intensities for C_{60}^{q+} ($q = 1$–3) to be determined should not be larger than those values in the present work drawn with solid circles in Fig. 6.

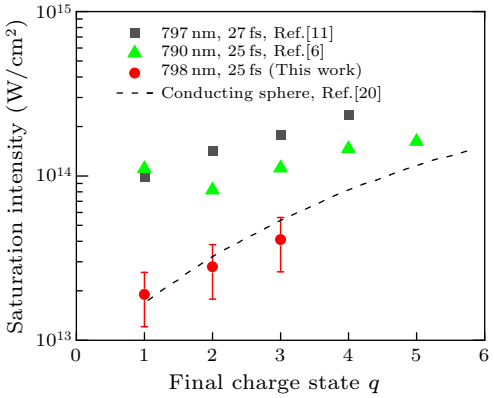

Fig. 6. Saturation intensity for C_{60} ionization to C_{60}^{q+} with short laser pulses as a function of the final charge state q. The data for 797 nm, 27 fs (squares) is taken from Fig. 5 of Ref. [11]; the data for 790 nm, 25 fs (triangles) is taken from Fig. 19 of Ref. [6] in which the authors derived them from Ref. [9]; the present data (circles); the estimated data using the conducting sphere model (dashed line) is taken from Fig. 2 (solid line) of Ref. [20].

A comparison between the present I_s values and the estimates by over-the-barrier ionization using the conducting sphere model of Bharadwaj *et al.*[20] is also shown in Fig. 6. The conducting sphere model fits our data fairly well. It should be noted that, although it nicely agrees with our data, the model is missing the centrifugal potential, which may strongly affect the generation of low charge states.[6] On the other hand, the TDDFT calculation by Bauer *et al.*[26] predicts a saturation intensity for the single ionization of C_{60} to be around 2×10^{13} W/cm^2, which is very close to our result. Detailed discussions for the rationality of the simulations are beyond the scope of our ability. Nevertheless, the current measurements provide alternative data which are helpful to reconsider those saturation intensities published theoretically and experimentally. In addition, in contrast to all other studies with a traditional TOFMS, the present measurements show detectable fragmentation even for excitation with 25 fs laser pulse at the intensity much lower than 1×10^{13} W/cm^2. This may be due to the fact that the signal-to-background ratio of the traditional approach is not sufficient to identify such weak fragmentation signals.

In summary, we have performed an experiment to revisit the intense-field C_{60} ionization and fragmentation induced by interactions of 25-fs, 798-nm laser pulses with a well-collimated C_{60} molecular beam, us-

ing a VMIS working in the time-sliced imaging mode. We demonstrate that the measured time-sliced photoion images show wonderful features in measuring the laser-intensity-dependent ionization and fragmentation yields of C_{60} molecules in a low intensity regime which has not been explored before. Such a revisit allows us to provide new insight into the intense-field ionization and fragmentation of C_{60}, at least in the following two points. One is that the derived saturation intensities for single, double, and triple ionizations of C_{60} and threshold for C_{60} fragmentation are much lower than those reported in previous experiments. The other is that the derived saturation intensities may imply the validity of the theoretical predictions by over-the-barrier ionization using the conducting sphere model.

References

[1] Dewitt M J and Levis R J 1998 *Phys. Rev. Lett.* **81** 5101
[2] Hankin S M, Villeneuve D M, Corkum P B and Rayner D M 2000 *Phys. Rev. Lett.* **84** 5082
[3] Lépine F 2015 *J. Phys. B: At. Mol. Opt. Phys.* **48** 122002
[4] Hunsche S, Starczewski T, L'Huillier A, Persson A, Wahlström C G, van den van L H B and Svanberg S 1996 *Phys. Rev. Lett.* **77**
[5] Campbell E E B and Levine R D 2000 *Annu. Rev. Phys. Chem.* **51** 65
[6] Schulz C P, Hertel I V and Laarmann T 2005 *Adv. Atom. Mol. Opt. Phys.* **50** 219
[7] Tchaplyguine M, Hoffmann K, Dühr O, Hohmann H, Korn G, Rottke H, Wittmann M, Hertel I V and Campbell E E B 2000 *J. Chem. Phys.* **112** 2781
[8] Hertel I V, Shchatsinin I, Laarmann T, Zhavoronkov N, Ritze H H and Schulz C P 2009 *Phys. Rev. Lett.* **102** 023003
[9] Campbell E E B, Hansen K, Hoffman K, Tchaplyguine M, Wittmann M and Hertel I V 2001 *J. Chem. Phys.* **114** 1716
[10] Bhardwaj V R, Corkum P B and Rayner D M 2004 *Phys. Rev. Lett.* **93** 043001
[11] Shchatsinin I, Laarmann T, Stibenz G, Steinmeyer G, Stalmashonak A, Zhavoronkov N, Schulz C P and Hertel I V 2006 *J. Chem. Phys.* **125** 194320
[12] Qian D B, Zhang X J, Zhang D C, Zhang S F, Yang J, Cheng R, Zhu X L and Ma X 2018 *Chem. Phys. Lett.* **691** 110
[13] Qian D B, Shi F D, Chen L, Martin S, Bernard J, Yang J, Zhang S F, Chen Z Q, Zhu X L and Ma X 2018 *J. Chem. Phys.* **148** 134303
[14] Zhou W C, Zhao D M, Qian D B, Li Y F, Y, Shi F D, Zhu Y H, Zhang S F, Zhu X L, Wu Y and Ma X 2019 *Int. J. Mass. Spectrom.* **440** 27
[15] Eppink A T J B and Parker D H 1997 *Rev. Sci. Instrum.* **68** 3477
[16] Spence D E, Kean P N and Sibbett W 1991 *Opt. Lett.* **16** 42
[17] Strickland D and Mourou G 1985 *Opt. Commun.* **56** 219
[18] Li Y F, Zhao D M, Zhou W C, Qian D B, yang J, Zhang S F, Zhu X L and Ma X 2019 *Int. J. Mass. Spectrom.* **442** 23
[19] Hankin S M, Villeneuve D M, Corkum P B and Rayner D M 2001 *Phys. Rev. A* **64** 13405
[20] Bhardwaj V R, Corkum P B and Rayner D M 2003 *Phys. Rev. Lett.* **91** 203004
[21] Jaroń-Becker A, Becker A and Faisal F H M 2006 *Phys. Rev. Lett.* **96** 143006
[22] Lezius M, Blanchet V, Rayner D M, Villeneuve D M, Stolow A and Ivanov M Y 2001 *Phys. Rev. Lett.* **86** 51
[23] Hansen K, Hoffmann K and Campbell E E B 2003 *J. Chem. Phys.* **119** 2513
[24] Hansch P and Van Woerkom L D 1996 *Opt. Lett.* **21** 1286
[25] Walker M A, Hansch P and Van Woerkom L D 1998 *Phys. Rev. A* **57** R701
[26] Bauer D, Ceccherini F, Macchi A and Cornolti F 2001 *Phys. Rev. A* **64** 063203